Glycopolymers as Antiadhesives of E. coli Strains Inducing Inflammatory Bowel Diseases

ARTICLE *in* BIOMACROMOLECULES · MAY 2015

Impact Factor: 5.75 · DOI: 10.1021/acs.biomac.5b00413 · Source: PubMed

16 AUTHORS, INCLUDING:

Redouane Borsali
French National Centre for Scientific Research
234 PUBLICATIONS **4,367** CITATIONS
SEE PROFILE

David Deniaud
University of Nantes
84 PUBLICATIONS **704** CITATIONS
SEE PROFILE

Julie Bouckaert
Université des Sciences et Technologies de Lill…
86 PUBLICATIONS **2,279** CITATIONS
SEE PROFILE

Julien Bernard
French National Centre for Scientific Research
78 PUBLICATIONS **1,209** CITATIONS
SEE PROFILE

Article

pubs.acs.org/Biomac

Glycopolymers as Antiadhesives of *E. coli* Strains Inducing Inflammatory Bowel Diseases†

Xibo Yan,[‡,§,◆,¶] Adeline Sivignon,[‡,∥,⊥] Nao Yamakawa,[#] Agnes Crepet,[§,◆,¶] Christophe Travelet,[○] Redouane Borsali,[○] Tetiana Dumych,[□] Zhaoli Li,[△] Rostyslav Bilyy,[□] David Deniaud,[▽] Etienne Fleury,[§,◆,¶] Nicolas Barnich,[∥,⊥] Arlette Darfeuille-Michaud,[∥,⊥] Sébastien G. Gouin,*[,▽] Julie Bouckaert,*[,#] and Julien Bernard*[,§,◆,¶]

[§]Université de Lyon, Lyon, F-69003 France

[◆]INSA-Lyon, IMP, Villeurbanne, F-69621 France

[¶]CNRS, UMR 5223, Ingénierie des Matériaux Polymères, Villeurbanne, F-69621, France

[∥]Clermont Université, UMR 1071, Inserm/Université d'Auvergne, 63000 Clermont-Ferrand, France

[⊥]INRA, Unité Sous Contrat 2018, 63000, Clermont-Ferrand, France

[#]Unité de Glycobiologie Structurale et Fonctionnelle (UGSF), UMR 8576, Université Lille 1, F-59655 Villeneuve d'Ascq Cedex, France

[○]Centre de Recherches sur les Macromolécules Végétales (CERMAV − CNRS UPR 5301), Université de Grenoble-Alpes, ICMG − CNRS FR 2607, PolyNat Carnot Institute, Arcane LabEx, 601 rue de la Chimie, 38041 Grenoble, France

[□]Institute of Cell Biology, NASU, Drahomanov Street 14/16, 79005 Lviv, Ukraine

[△]Division of Bacterial Diseases, State key Laboratory of Veterinary Biotechnology, Harbin Veterinary Research Institute, Chinese Academy of Agricultural Sciences, Maduan St. 427#, Nangang Dis, Harbin, China

[▽]LUNAM Université, CEISAM, Chimie Et Interdisciplinarité, Synthèse, Analyse, Modélisation, UMR CNRS 6230, UFR des Sciences et des Techniques, 2, rue de la Houssinière, BP 92208, 44322 Nantes Cedex 3, France

Supporting Information

ABSTRACT: *n*-Heptyl α-D-mannose (HM) is a nanomolar antagonist of FimH, a virulence factor of *E. coli*. Herein we report on the construction of multivalent HM-based glycopolymers as potent antiadhesives of type 1 piliated *E. coli*. We investigate glycopolymer/FimH and glycopolymer/bacteria interactions and show that HM-based glycopolymers efficiently inhibit bacterial adhesion and disrupt established cell−bacteria interactions in vitro at very low concentration (0.1 μM on a mannose unit basis). On a valency-corrected basis, HM-based glycopolymers are, respectively, 10^2 and 10^6 times more potent than HM and D-mannose for their capacity to disrupt the binding of adherent-invasive *E. coli* to T84 intestinal epithelial cells. Finally, we demonstrate that the antiadhesive capacities of HM-based glycopolymers are preserved ex vivo in the colonic loop of a transgenic mouse model of Crohn's disease. All together, these results underline the promising scope of HM-based macromolecular ligands for the antiadhesive treatment of *E. coli* induced inflammatory bowel diseases.

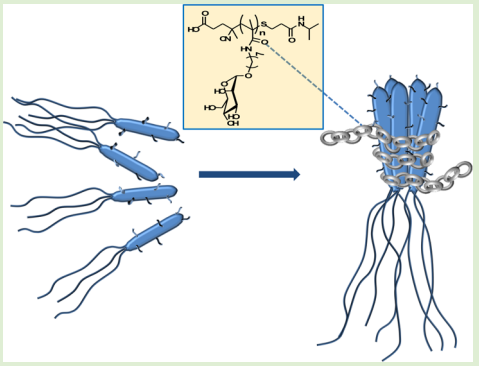

INTRODUCTION

Adhesion of bacterial pathogens to host cells and tissues, a prerequisite for a majority of infection diseases, is governed by interactions between bacteria surface lectins and complementary carbohydrates displayed at the host cell periphery. To promote adhesion and infection of tissues through multivalent interactions, bacteria such as *Escherichia coli* (*E. coli*) express hundreds of adhesive proteinaceous hair-like organelles, type 1 fimbriae, on their cell surface. These type 1 fimbriae are cylindrical rod-shaped extensions on the *E. coli* cell wall constituted of a major pilin subunit, FimA, followed by a short, flexible tip fibrillum composed of minor pilins FimF, FimG, and the adhesin FimH. The latter is exposed at the extremity of the fimbriae, and its lectin domain possesses a mannose-specific receptor site responsible for recognition and binding to host cells.[1] An overgrowth of *E. coli* is associated with infections, that is, urinary tract and bladder infections, inflammatory bowel diseases, sepsis, and meningitis, which usually require antibiotic treatments. As bacterial resistance to antibiotics is becoming a serious threat to public health, the antiadhesive therapy, which lies in the use of drugs capable of preventing the bacterial adhesion step with no bactericidal effect, is progressively

Received: March 27, 2015
Revised: April 29, 2015
Published: May 11, 2015

DOI: 10.1021/acs.biomac.5b00413
Biomacromolecules 2015, 16, 1827−1836

Scheme 1. Principle of HM-Based Glycopolymers Anti-Adhesive Action[a]

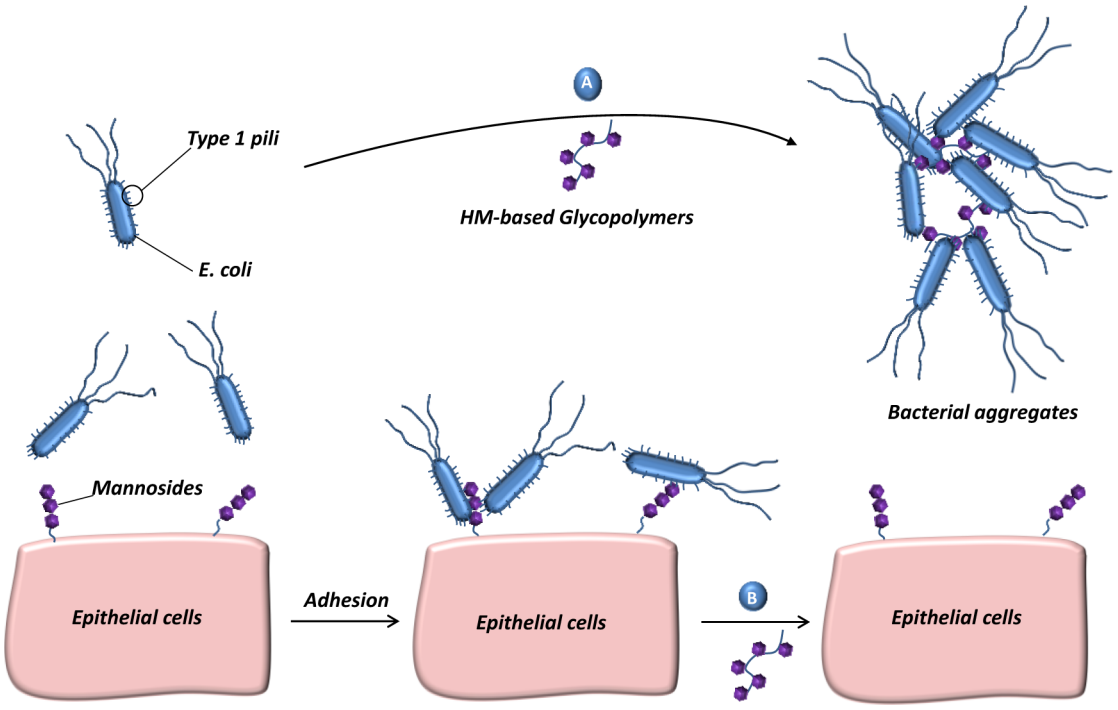

[a](A) Sequestration of free bacteria in the lumen of the gut; (B) Disruption of established *E coli*−cell interactions.

emerging as a valuable alternative.[2] Because carbohydrate−protein interactions are intrinsically weak (K_d typically in the mM to μM range), the applicability of this approach requires to develop compounds with high affinity toward bacterial lectins so that adhesion (and thus infections) can be prevented at reasonably low concentrations. In this context, extensive research has been carried out on the design of synthetic molecular inhibitors displaying structures that optimize interactions with the lectin sugar-binding site(s) to outmatch interactions with natural ligands. The feasibility of this approach has been demonstrated for *E. coli*. In their pionnering work, Sharon and co-workers showed that mannosides bearing aromatic aglycons are more efficient FimH inhibitors than the methyl mannoside reference.[3] X-ray structure investigations on FimH lectin cocrystallized with butyl α-D-mannoside highlighted that in addition to the hydroxyl groups of D-mannose, which establish hydrogen bonds with the amino acids located at the bottom of the FimH binding pocket, the butyl group develops strong hydrophobic interactions at the entrance (of the binding pocket), the so-called tyrosine gate (Tyr48, Ile52, and Tyr137).[4] Optimization of the alkyl chain length led to the discovery of *n*-heptyl α-D-mannose (HM), a nanomolar FimH antagonist (binding affinity of 5 nM recorded by SPR).[4] These findings greatly impacted the development of FimH antagonists paving the way to the discovery of other potent compounds with biphenyl,[5−7] indolinyl phenyl,[8] or squarate aglycones[9] for the potential treatment of *E. coli*-induced urinary tract infections. Recently, some of us also showed that thiazolylaminomannosides,[10] a new family of FimH antagonists, could extend the antiadhesive concept to the treatment of specific inflammatory bowel diseases such as Crohn's disease (CD), in which Adherent Invasive *Escherichia coli* (AIEC) can play a key role in the inflammation process.[11,12] Targeting the cause of the inflammation is a promising alternative to the current marketed CD drugs essentially based on lowering tumor necrosis factor (TNF) levels.[13]

Another conventional route for the design of high-affinity ligands consists in the incorporation of several epitopes on a common scaffold (multivalent molecule, dendrimer, or polymer chain).[14−23] Such derivatives can display noticeable enhancement in activity compared to their monovalent counterparts on a per mole of epitope basis on a wide range of lectins. This trend is often referred to as the "cluster glycoside" effect.[24] Multivalent FimH antagonists have been reported by several research groups. In seminal works, Lindhorst[25] and Roy[26,27] developed multivalent FimH inhibitors from dendrimer scaffolds, whereas Gouin and Bouckaert recently introduced HM ligands on functionalized hydrophilic cyclodextrin-based scaffolds and observed substantial cluster effects in vitro[28,29] and in vivo.[30]

In this contribution, we report on the preparation of potent macromolecular antiadhesives of type 1 piliated *E. coli* through the association of a judicious ligand selection with the presentation of multiple ligands on a polymeric scaffold. More precisely, we focus on the design of model macromolecular inhibitors of type-1 fimbriae bacterial adhesion based on the incorporation of multiple copies of *n*-heptyl α-D-mannose (HM), one of the strongest molecular binders of the monovalent lectin domain of FimH,[4] as pendent motifs. Herein we evaluate the capability of precisely defined HM-based glycopolymers to efficiently bind to FimH lectin domains of *E. coli* strains (UTI 89 and AIEC LF82 clinically isolated from patients with urinary tract infections and Crohn's disease, respectively) and to prevent or disrupt adherent-invasive *E. coli* adhesion with live epithelial cells in vitro and ex vivo at very low concentration on a mannose unit basis (Scheme 1).

EXPERIMENTAL SECTION

Materials. *Chemical Reagents.* All reactants, unless stated otherwise, were purchased from Sigma-Aldrich. The solvents were purchased from Carlo Erba. HM, HMM, and EMM were synthesized as described in the literature.[4,31]

DOI: 10.1021/acs.biomac.5b00413
Biomacromolecules 2015, 16, 1827−1836

Intestinal Epithelial Cells. Human intestinal epithelial cell line T84 and human cervical adenocarcinoma cell line HeLa were purchased from American Type Culture Collection (ATCC, CCL-248; ATCC, CCL-2) and maintained in the culture medium recommended by ATCC in an atmosphere containing 5% of CO_2 at 37 °C. Human colorectal adenocarcinoma cell line Caco-2 was obtained from the Cell Culture Collection of the Department of Structural and Functional Glycobiology, Faculty of Biology, University of Science and Technology of Lille 1. Cells were cultured in EMEM medium supplemented with 20% fetal bovine serum (FBS) and penicillin/streptomycin.

Construction of Fluorescent Strain UTI89 nadB::cat-kat. The strain LF82 nadB::cat-kat was constructed with the recombination system reported by Datsenko and Wanner[32] except that the linear fragments used were long homologous recombinant sequences amplified from pDONR221-nadB-catkat derived from pDONR221-nadB.[33] Briefly, the recombinant plasmid pDONR221-nadB-cat was constructed first by amplification of the chloramphenical gene from pKD3[32] using the primers EcatF GCAATGAATTCTAGAGAATA-GGAACTTCGGAAT and EBcatR (ATTGCGAATTC*GGATCC*-AAGTATAGGAACTTCGGCGCGCCTA), enzymatic digestion by *Eco*RI and ligation into pDONR221-nadB. The katushka gene *kat* were amplified with primers KatF, containing the *Bam*HI site and em7 promoter sequences (CGC*GGATCC*TGTTGACAATTAATCA-TCGGCATAGTATATCGGCATAGTATAATACGACAAGGTGA-GGAACTAAACCATGGTGGGTGAGGATAGCGTGCTGA) and KatR (CGC*G GATCC*GCATTAGCTGTGCCCCAGTTT) from pTurboFP-635C (Evrogen). The fragments and the pDONR221-nadB-cat were digested using *BamH1*. Upon ligation, the plasmid pDONR221-nadB-cat-kat was obtained. The plasmid was transformed into *E. coli* LF82 and clones containing the plasmid selected on kanamycin/chloramphenicol LB-agar during an overnight incubation at 37 °C. Incubation during another 4 days at room temperature showed pink colonies, confirming the expression of the katushka near-infrared fluorescent protein.

Enzyme-Linked Lectinosorbent Assay. Enzyme-linked lectinosorbent assay (ELLSA) was performed using microplate reader BioTek-ELx800. RNase B proteins (Sigma, R-7884) were used as a substrate of oligomannose glycans. For detection of FimH binding toward nature glycans were used rabbit anti-FimH polyclonal antibodies (Eurogentec) and goat antirabbit HRP-labeled secondary antibody (Enzo Life Sciences).

E. coli strain LF82 isolated from an ileal biopsy of a CD patient was used as AIEC reference strain.[11] Bacteria were grown overnight at 37 °C in Luria−Bertani (LB) broth. A bacterial suspension was prepared in phosphate buffer saline (PBS) for in vitro adhesion assays or ex vivo assays on colonic mucosa from CEABAC10 mice.

Characterization Methods. *Nuclear Magnetic Resonance.* Nuclear magnetic resonance (NMR) spectra were recorded on a Bruker Avance III spectrometer (400 MHz) in $CDCl_3$ (for monomer precursors and multifunctional RAFT agents) or D_2O solutions (glycomonomers, glycopolymers) at 298 K and referenced to residual solvent peaks. ESI-MS spectra (m/z) of monomer precursors, glycomonomers, and RAFT agents were measured on a Thermo-FinniganMat 95XL.

Aqueous Size Exclusion Chromatography and Light Scattering. Aqueous size exclusion chromatography (SEC) analysis of glycopolymers was performed in a 0.1 M $NaNO_3$ aqueous solution (pH adjusted to 7 by addition of NaOH) at a flow rate of 0.5 mL/min at 22 °C. This system was composed of an isochrom LC pump with autosampler Water 717, a multiangle laser light scattering (MALLS) detector (Wyatt EOS) was coupled online with a differential refractometer Wyatt Optilab T-rex (λ = 658 nm) and with two PL aquagel OH mixed H and M columns (Agilent). For light scattering measurements, dn/dc coefficients were calculated with a laser source operating at 658 nm. dn/dc values were determined from the slopes of curves plotting the variation of the refractive index as a function of the concentration (dn/dc = 0.172). Acetylated glycopolymers were analyzed with a SEC apparatus running in THF at 25 °C (flow rate: 1 mL·min^{-1}) and equipped with a Viscotek VE 1121 automatic injector, three columns (Waters HR2, HR1, and HR0.5), and a differential refractive index detector (Viscotek VE3580). The average molar masses of the glycopolymers were derived from a calibration curve based on a series of PS standards.

The light scattering study on FimH/L188 interactions was performed using an ALV/CGS-8FS/N069 apparatus (from ALV) equipped with an ALV/LSE-5004 multiple τ digital correlator with a 125 ns initial sampling time (from ALV) and a 35 mW red helium−neon linearly polarized laser operating at a wavelength of 632.8 nm (from JDSU). Both suspensions and their resulting mixture were used unfiltered. The studied systems were loaded in 10 mm diameter cylindrical cells, immerged in a toluene bath and thermostated at a temperature of 25.0 ± 0.1 °C prior to measurements. Data were collected at different scattering angles ranging from 14 to 143° by step of 1° for a counting time of typically 60 s using the digital ALV correlator control software. In dynamic light scattering (DLS), the relaxation time distribution was obtained using the Contin analysis of the autocorrelation function ($g^{(2)}$-1). In static light scattering (SLS), the scattering intensity was corrected by the solvent signal and normalized by the toluene signal. The scattering volume change with observation angle was also taken into account.

Additional DLS experiments on glycopolymer/FimH interaction (see Supporting Information) were performed by a Malvern Instruments Zetasizer nano series instrument using the cumulant method with aqueous solution of glycopolymer and FImH (see Supporting Information) in Hepes buffer at 20 °C. Specifically, FimH aqueous solution (83 μM) were prepared and measured by DLS with protein workspace mode. The glycopolymer aqueous solution was progressively added into FimH solution, DLS data was recorded after each addition to follow the formation of glycopolymer/FimH aggregates. At least three measurements were made for each sample. Equilibration times of 5 min were respected before each measurement.

Microscopy Techniques. In order to perform Atomic Force Microscopy measurements, silicon substrates (approximately 1 × 1 cm^2) were cleaned by ozonolysis treatment. Samples were prepared by spin-coating (4000 rpm, 30 s) from aqueous solutions of L188 and FimH (at the concentrations given in the main text) and dried under vacuum. AFM images were acquired in air at room temperature using a Nanoscope IIIa Multimode (Digital Instruments/VEECO, CA). Intermittent contact imaging (i.e., tapping mode) was performed at a scan rate of 1 Hz. Uncoated silicon probes with a resonant frequency between 280 and 405 kHz, a spring constant 20 and 80 N/m, length of 115−135 μm, width of 30−40 μm, and nominal tip radius of curvature less than 10 nm are used. Images were displayed and analyzed using the Nanoscope 6.14R1 software.

Fluorescent microscopy was performed with fixed slides under a Carl Zeiss AxioImager A1 DIC/fluorescent microscope (Oberkochen, Germany) using 0.4 NA 10× , 0.75 NA 40× air, and 1.3 NA 100× oil immersion objectives. Fluorescent images were taken by a Zeiss AxioCam MRmIII cooled digital CCD camera under constant exposure. Fluorescence of katushka was evaluated at red channel (610 nm emission was obtained at 532 nm excitation) and at similar conditions the emission at NIR channel (700 nm) was detected. Zeiss AxioVision and ImageJ software were used for image analysis.

Synthetic Procedures. *Synthesis of CPADB-Based Trifunctional RAFT Agent.* In a preliminary step, an activated RAFT agent was prepared as previously reported.[34] Typically, in an argon conditioned Schlenk tube, 4-cyano-4-(phenylcarbonothioylthio) pentanoic acid (CPADB, 297 mg, 1 mmol) was dissolved in chloroform (20 mL). After cooling to 0 °C, *N*-hydroxysuccinimide (115 mg, 1 mmol) and *N*,*N*′-dicyclohexylcarbodiimide (206 mg, 1 mmol) were successively added. After 1 h at 0 °C, the solution was stirred overnight at room temperature. The solution was filtrated, and the solvent was evaporated to afford the activated RAFT agent as a pink powder (95%, 357 mg). ^{1}H NMR (250 MHz, $CDCl_3$) δ 7.91 (d, J = 7.5 Hz, 2H, phenyl), 7.58 (t, J = 7.5 Hz, 1H, phenyl), 7.41 (t, J = 7.5 Hz, 2H, phenyl), 3.11−2.45 (m, 8H, CH_2CH_2CO and CCH_2CH_2C), 1.96 (s, 3H, CH_3). ^{13}C NMR ($CDCl_3$) δ 220.01, 168.93, 167.22, 144.52, 133.31, 128.76, 126.87, 118.28, 45.59, 32.88, 27.05, 25.71, 24.38 (see Supporting Information).

DOI: 10.1021/acs.biomac.5b00413
Biomacromolecules 2015, 16, 1827−1836

The activated RAFT agent (1.24g, 3.3 mmoL) was dissolved in THF (100 mL), and a solution of tris(2-aminoethyl)amine (146 mg, 1 mmol) in methanol (10 mL) was added dropwise at room temperature. The solution was stirred for 1h. After reaction, the solvent was evaporated and the crude product was purified by column chromatography (CH_2Cl_2/methanol, 30/1, v/v); 520 mg (41%) as pink powder. ^{1}H NMR (250 MHz, $CDCl_3$) δ 7.86 (m, 6H, phenyl), 7.53 (m, 3H, phenyl), 7.35 (m, 6H, phenyl), 6.93 (s, 3H, N*H*), 3.29 (s, 6H, NHCH_2CH_2N), 2.88−2.21 (m, 18H, CH_2CH_2CO and NHCH_2CH_2N), 1.90 (m, 9H, CH_3). ^{13}C NMR ($CDCl_3$) δ 222.89 (SCS), 171.43 (CONH), 144.61, 133.16, 128.70, 126.85 (phenyl), 118.94 (*C*N), 54.80 (NCH_2CH_2), 46.34 (CH_3CCN), 38.23 (NCH_2CH_2NH), 34.36 (COCH_2CH_2), 31.88 (CH_2CH_2C), 24.23 (CH_3) (see Supporting Information). ESI-MS: m/z Calcd for $C_{45}H_{52}N_7O_3S_6$ $[M + H]^+$, 930.2450; found, 930.2409.

Synthesis of CPADB-Based Octafunctional RAFT Agent. To a solution of Octa Ammonium POSS purchased from Hybrid Plastics (200 mg, 0.17 mmol) in methanol (10 mL) was added 0.33 mL of DIPEA (2 mmol). After 2 h under stirring, the solution was introduced drop by drop in a solution of activated RAFT agent (650 mg, 1.7 mmoL in 100 mL) of THF. After 1 h of reaction, the solvent was evaporated and the RAFT agent was finally purified by column chromatography (CH_2Cl_2/methanol, 30/1, v/v) to obtain a pink powder (151 mg, 30%). ^{1}H NMR (250 MHz, $CDCl_3$) δ 7.88 (d, J = 7.5 Hz, 16H, phenyl), 7.54 (t, J = 7.5 Hz, 8H, phenyl), 7.37 (t, J = 7.5 Hz, 16H, phenyl), 6.56 (s, 8H, N*H*), 3.45−3.22 (m, 16H, CH_2CH_2NH), 2.75−2.24 (m, 32H, CH_2CH_2CO), 1.89 (s, 24H, CH_3), 1.78−1.45 (m, 16H, SiCH_2CH_2), 0.78−0.52 (m, 16H, SiCH_2CH_2). ^{13}C NMR ($CDCl_3$) δ 222.89 (SCS), 170.94 (CONH), 144.64, 133.21, 128.74, 126.84 (phenyl), 118.95 (*C*N), 46.33 (CH_3CCN), 42.19 (NHCH_2CH_2), 34.35 (COCH_2CH_2), 31.98 (CH_2CH_2C), 29.83 (CH_2CH_2CH_2), 24.28 (CH_3), 23.02 (CH_2CH_2CH_2) (see Supporting Information). ESI-MS: m/z Calcd for $C_{128}H_{154}N_{16}O_{20}S_{16}Si_8$ $[M + 2H]^{2+}$, 1485.2600; found, 1485.2639.

RAFT Polymerizations. In a typical experiment, a Schlenk flask (10 mL) was charged with monomer HMM (100 mg, 2.80 × 10^{-4} mol) dissolved in 0.37 mL of water, 4,4′-azobis(4-cyanovaleric acid) (ACPA, 0.52 mg, 1.85 × 10^{-6} mol), and 4-cyano-4-(phenylcarbonothioylthio) pentanoic acid (1.56 mg, 5.55 × 10^{-6} mol) dissolved in 0.37 mL of DMSO. After mixing, the pink solution was deoxygenated by three consecutive freeze−pump−thaw cycles. After the last cycle, the Schlenk flask was filled with nitrogen, allowed to warm to room temperature and finally immersed in an oil bath at 70 °C. After polymerization (conversion at 84%), the Schlenk flask was plunged into iced water and the solution was then freeze-dried overnight. The crude product was redissolved in a minimal quantity of solvent (methanol/DMSO, v/v, 20/1) and precipitated in an acetone/petroleum ether mixture (v/v, 7/3) to remove unreacted monomer and initiator. The resulting pink powder was dried overnight under vacuum to give 60 mg of L47 as a pale pink solid. M_{nSEC} = 17.9 kg mol^{-1}, $Đ$ = 1.03 (^{1}H NMR spectrum given in Figure S9). Kinetics of polymerization and SEC traces of the resulting linear glycopolymers are given in Supporting Information.

Polymerizations of HMM in the presence of CPADB-based trifunctional RAFT agent were carried out in similar conditions. Polymerizations of HMM in the presence of CPADB-based octafunctional RAFT agent were carried out in pure DMSO using AIBN as initiator owing to the poor solubility of the RAFT agent in water. Kinetics of polymerization and SEC traces of the resulting star-shaped glycopolymers are given in Supporting Information.

Removal of the Dithiobenzoate Chain Ends. HM-based glycopolymer (L47, 40 mg, 2.32 × 10^{-6} mol) was dissolved in 1 mL of DMSO (1 mL). The solution was deoxygenated by three consecutive freeze−pump−thaw cycles. Ethanolamine (1.4 mg, 10 equiv) was added in solution and the pink color immediately disappeared. NIPAAm (13.2 mg, 50 equiv) and dimethylphenylphosphine (0.3 mg, 1 equiv) were then incorporated and the solution was stirred overnight at room temperature. Water (2 × 100 mL) and dichloromethane (200 mL) were added to the solution. The aqueous phase was collected, dialyzed against deionized water for 2 days, and freeze-dried to afford a fluffy white powder (36 mg, 90%).

Acetylation of HM-Based Glycopolymers for SEC Analysis in THF. The glycopolymer (L47, 2 mg, 1.16 × 10^{-7} mol) was dissolved in a solution of anhydrous DMF (1 mL) containing pyridine (4.3 mg, 2 equiv per hydroxyl group). Acetic anhydride (14.0 mg, 5 equiv per hydroxyl group) was incorporated into the solution. The solution was heated overnight at 50 °C. After reaction, 150 mL of dichloromethane was added. The solution was washed with water (2 × 200 mL) and dried by $MgSO_4$, and the solvent was evaporated to obtain the acetylated glycopolymer (yield ∼ 90%) as a beige paste.

Cytotoxicity Tests. The cytotoxicity tests were performed using FACS Calibur flow cytometer (BD Biosciences, San Jose, CA, U.S.A.) according to manufacturers' instructions and generally accepted procedures. Propidium iodide (PI) was used to counterstain necrotic cells (PI+). Apoptotic cells were detected as Annexin-V-FITC+/PI- cells.

Competitive Enzyme-Linked Lectinosorbent Assay (ELLSA). Immunosorbent microplates (Nunc, Maxisorp) were coated with 100 μL of 5 mg/mL solution of RNase-B in 100 mM carbonate/bicarbonate buffer pH 9.6. Plates were incubated at 4 °C overnight and then washed (300 μL/well) three times with 10 mM phosphate−buffered saline (PBS) containing 0.15% Tween-20. All wells were blocked with 200 μL 3% bovine serum albumin (BSA) in 10 mM phosphate−buffered saline (PBS) containing 0.15% Tween-20 (PBST) and incubated at 37 °C for 2 h. Then it was washed three times with PBST. Mannosides were dissolved in PBST at the concentrations indicated on graphs and added to the microwells. FimH was diluted in PBST to 0.07 μM and added to each well of plate and incubated for 1h at room temperature. Wells were washed three times with PBST. Wells were incubated with 100 μL of rabbit-anti-FimH antibodies IgG (aFimH) diluted 1:5000 in PBST for 1 h at room temperature. Wells were washed three times with PBST and incubated with 100 μL of goat-antirabbit HRP-labeled secondary antibody, Enzo Life Sciences (2ndAb-HRP) diluted 1:10000 in PBST for 1 h at room temperature. The wells were washed three times with PBST and 100 μL of 3,3′,5,5′-tetramethylbenzidine (TMB) were added to each well and incubated in darkness for 5−15 min. The reaction was stopped with 100 μL/well of 1N sulfuric acid. Plate absorbance was analyzed at 450 nm using microplate reader BioTek-ELx800.

Adhesion Tests. *Detailed Procedures on Experiments with Katushka UTI89 + L188 and with Caco-2/HeLa with LF82 and L188.* To evaluate the effectiveness of the glycopolymers, we used the model of coincubation of Crohn's disease provoking strain LF82 of *E. coli* bacteria with human epithelia cells of Caco-2 and HeLa cell lines. Cells were grown on the glass. Before adding of a bacterial suspension, cells were washed three times by fresh culture medium (without antibiotic). A 4 μL bacterial suspension of type 1 piliated *E. coli* strain LF82 ($OD_{650\ nm}$ = 1.3) was added to cells. L188 inhibitor was added at concentration of 500 nM. After 2 h of coincubation of cells with bacteria (in the presence or absence of L188 inhibitor), samples were analyzed by fluorescent microscopy.

Adhesion Assays of AIEC LF82 Strain on Intestinal Epithelial Cells T84. The intestinal epithelial cells T84 were seeded in 48-well tissue culture plates at a density of 1.5 × 10^5 cells/well and were incubated at 37 °C for 48h. For preincubation protocol, AIEC LF82 bacteria were incubated for 1 h with mannoside derivatives (α-D-Mannose, HM or HMM) or HM-based glycopolymers at final concentrations of 1, 0.1, and 0.01 μM (in mannose unit basis, corresponding for L188 to 340, 34, and 3.4 ng·mL^{-1}, respectively) then cells were infected with the mixture at a multiplicity of infection (MOI) of 10 bacteria per cell for 3 h. Monolayers were washed 3 times with phosphate buffer (PBS) and lysed with 1% Triton X-100 (Sigma) in deionized water. Samples were diluted and plated onto LB agar plates to determine the number of colony-forming units (CFU). For the postincubation protocol, cells were infected with AIEC LF82 bacteria at a MOI of 10 for 3 h, then monolayers were extensively washed with PBS and inhibitory compounds were added at final concentrations of 10, 1, and 0.1 μM (in mannose unit basis) onto the cells for an additional 3 h period.

DOI: 10.1021/acs.biomac.5b00413
Biomacromolecules 2015, 16, 1827−1836

Table 1. Linear and Star-Shaped PHMM Glycopolymers Obtained by RAFT Polymerization

PHMM	topology	M_n[a] (kg mol^{-1})	DP_n[b]	D_h[c] (nm)
L31	linear	11.5	31	4.2
L47	linear	17.2	47	5.0
L55	linear	20.2	55	5.2
L69	linear	25.3	69	5.9
L106	linear	38.6	106	6.5
L188	linear	68.4	188	7.9
T51	3-arm star	19.6	51	5.9
T74	3-arm star	28.0	74	6.4
T93	3-arm star	34.8	93	6.5
T200	3-arm star	73.2	200	8.0
O74	8-arm star	29.7	74	6.4
O269	8-arm star	100.4	269	9.1

[a]Overall DP determined from relative integration of the aromatic chain end group and polymer backbone peaks. [b]Determined from DLS analysis in pure water. [c]Samples prone to aggregate.

Ex Vivo Assay: Adhesion Assays of AIEC LF82 Strain on Colonic Tissues from CEABAC10 Mice. Adhesion assay of AIEC LF82 bacteria were performed using colonic tissues from transgenic mice expressing the human CEACAM6 protein.[35] Briefly, 10−12-week-old FVB/N CEABAC10 transgenic mice were anesthetized, euthanized by cervical dislocation and colons were removed. Colons were washed twice in phosphate buffer saline (PBS) and segmented in independent loops of ≈0.6 cm. A volume of 100 μL containing 6×10^5 CFU of LF82 bacteria in PBS in the presence or absence of 3.4 μmol of the glycopolymer L188 were injected into the loops. Loops were incubated 4 h at 37 °C in Krebs-Ringer bicarbonate buffer (Sigma) in an atmosphere containing 5% of CO_2, and then opened and washed (four times) in PBS. Tissues were homogenized, appropriately diluted, and plated onto Luria−Bertani agar plates containing ampicillin (100 μg/mL) and erythromycin (20 μg/mL) to select AIEC LF82 bacteria.

RESULTS AND DISCUSSION

Macromolecular FimH antagonists with different size and topology were designed to assess the influence of HM valency and spatial presentation of the epitopes. We hypothesized that the polymeric antagonists would generate stronger multivalent interactions, on a valency-corrected basis, by recruiting a higher number of bacterial pili, mimicking more accurately *E. coli* attachment to the glycocalyx of the host cells. In a preliminary step, *N*-[7-(α-D-mannopyranosyloxy)heptyl]methacrylamide] (HMM),[31] a HM-based monomer was polymerized in the presence of 4-cyanopentanoic acid dithiobenzoate (CPADB) or CPADB-based multifunctional CTAs to generate a set of precisely defined linear and 3-arm or 8-arm star glycopolymers with valencies ranging from 31 to 269 (L31 and O269, respectively, L31 being a linear PHMM with a DP_n = 31 and O269 a 8-arm star PHMM with a DP_n = 269) and hydrodynamic diameters varying from 4.2 to 9.1 nm (see Table 1 and Scheme 2, as well as Figures S1 and S2 and Table S1 for polymerizations details and molar mass characterizations).

Dithiobenzoate end groups were then removed through aminolysis/capping steps to overcome cytotoxicity issues (conclusive cytotoxicity tests on human intestinal epithelial Caco-2 cells given in Figure S3).

Scheme 2. Molecular/Macromolecular FimH Antagonists Synthesized and Tested

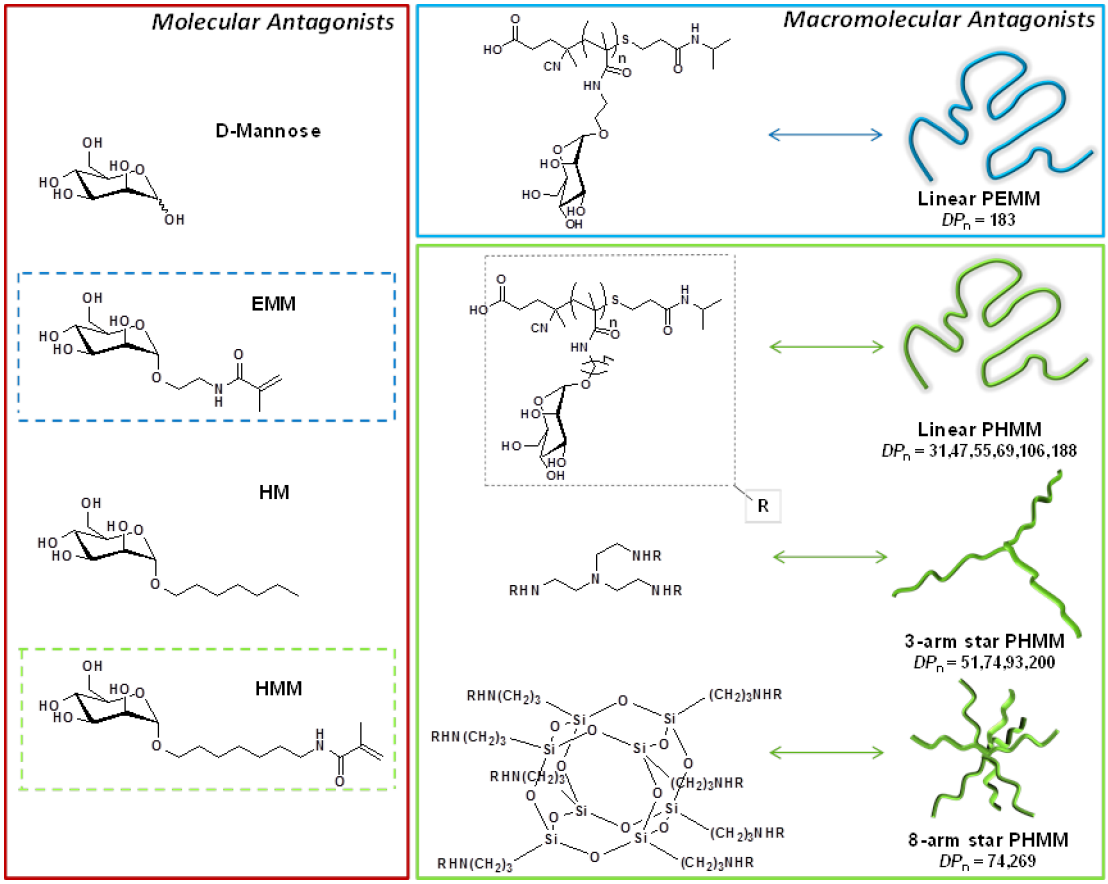

DOI: 10.1021/acs.biomac.5b00413
Biomacromolecules 2015, 16, 1827−1836

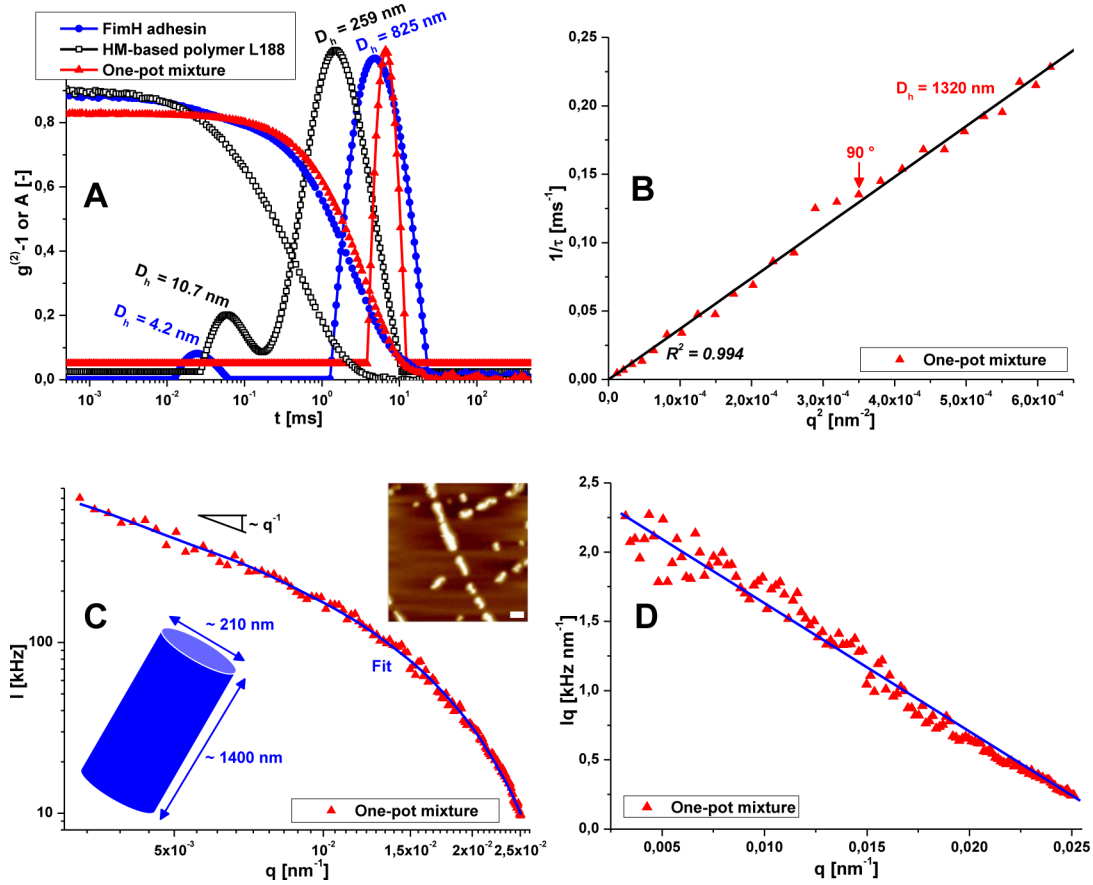

Figure 1. (A) DLS, autocorrelation function ($g^{(2)}$-1), and relaxation time distribution (A) at 90°; (B) DLS, inverse of the relaxation time distribution maximum ($1/\tau$) on squared wave vector modulus (q^2) between 15 and 140° by steps of 5° (hydrodynamic diameter (D_h), and correlation coefficient (R^2)); (C) SLS, scattering intensity (I) on wave vector modulus (q) between 14 and 143° by steps of 1°; Inset: AFM picture of FimH-L188 complexes (scale bar: 1 μm); (D) SLS, corresponding Kratky plot. All measurements were carried out in HEPES buffer (20 mM, pH 7.4) containing NaCl (150 mM).

To gain preliminary insight into type 1 piliated *E. coli* bacteria/PHMM interactions, association of FimH adhesin and glycopolymer chains was investigated by dynamic light scattering (DLS). To closely apprehend the initial conditions, DLS was first carried out on FimH adhesin (83 μM) on the one hand and PHMM (L188, 15 μM) on the other hand (Figure 1A, blue and black curves, respectively). The D_h values, 4.2 ± 0.1 and 825 ± 33 nm, are obtained for FimH adhesin and 10.7 ± 0.3 and 259 ± 2 nm for L188, corresponding to free macromolecules and preassembled ones. The diameter of gyration (D_g) of 68.4 kg mol^{-1} glycopolymer (DP_n = 188) in Θ-solvent conditions is crudely given, taking into account the polymer pending groups, by $D_g = 2(DP_n b^2/6)^{1/2} \sim 12$ nm, where b gives the segment length ($b \sim 7 \times 0.154$ nm). This calculated value is compatible with the experimental value 10.7 nm, thus, showing the presence of single molecule coils. The molar mass of FimH adhesin (16.9 kg mol^{-1}) is also coherent with the experimental value 4.2 nm. The distributions shown in Figure 1A are mass-weighted. When converting them into number-weighted distributions, we get $N_{small} \sim 10^3$–10^5 N_{big}, meaning that the number of free macromolecules (N_{small}) is in fact much larger than that of preassembled ones (N_{big}). A polymer suspension of L188 (20 μL at 15 μM) was subsequently added in a single step to a suspension of FimH adhesin (350 μL at 83 μM, [Man]/[FimH] ~ 2). The above-mentioned populations almost instantaneously disappear upon addition, replaced by a new single narrow-sized population (Figure 1A, red curve), which can be reasonably attributed to the formation of FimH adhesin/PHMM complexes (the association of FimH with PHMM chains was confirmed for all the polymers given in Table 1, see Supporting Information). These self-assemblies were probed by DLS at various scattering angles from 15 to 140° (Figure 1B). The inverses of the relaxation time distribution maxima ($1/\tau$) exhibit a proportional dependency with q^2 (squared wave vector modulus), displaying Brownian diffusive motion of objects characterized by the D_h-value of 1320 nm. Static light scattering (SLS) was carried out on this peculiar mixture (Figure 1C). Experimental scattering intensity perfectly fits with the form factor of uniform cylinder of length about 1400 nm and diameter about 210 nm (blue solid line, Figure 1C). Accordingly, a single linear regime is observed on the Kratky representation (Figure 1D). These results are further corroborated by atomic force microscopy (AFM) measurements where the cylinder length and diameter in the dried state coincide with the values determined by SLS in aqueous solution (see inset Figure 1C). The formation of these original supramolecular cylinders thus demonstrates the capability of each glycopolymer chain to accommodate a large number of FimH adhesin molecules. The capability of PHMM chains to bind FimH in their natural environment, that is, when the lectin is located to the extremity of bacteria pili, was then investigated. In this view, a bacterial suspension of type

DOI: 10.1021/acs.biomac.5b00413
Biomacromolecules 2015, 16, 1827–1836

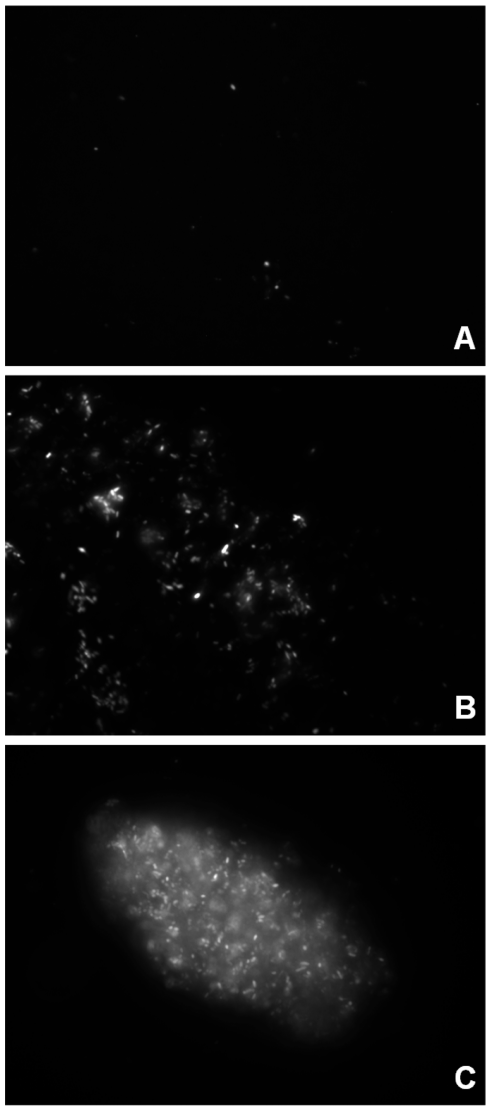

Figure 2. Glycopolymer-induced agglutination of type 1 fimbriated *E. coli* (strain UTI89). (A) Fluorescence microscopy pictures of Katushka-expressing type 1 fimbriated *E. coli* UTI89; (B) exposed to 1 μM of L188; (C) to 3 μM of L188 and resulting in a "bacterial egg" agglomerate with approximate dimensions 98 × 51 μm.

1 piliated *E. coli* strain UTI89 ($OD_{650\ nm}$ = 1.3) was subjected to PHMM chains at concentrations ranging from 1 to 3 μM of L188 (see Figure 2). As shown in Figure 2B,C, PHMM acts as a powerful glue to agglutinate *E. coli* bacteria. Introduction of PHMM results in the formation of bacterial clusters whose size increases with the concentration of glycopolymer chains (50 × 98 μm after adding 3 μM), confirming that the glycopolymer chains induce multiple binding events with the bacteria-bound FimHs and that one glycopolymer chain is capable of establishing cross-linking interactions with FimH adhesins expressed by multiple bacteria.

The propensity of the glycopolymers to prevent attachment of *E. coli* to host cells was further investigated through adhesion assays (Figure 3). Infections of intestinal epithelial T84 cells were performed with AIEC reference strain LF82 previously incubated with a series of mannosides (HMM, HM and α-D-mannose) or PHMM (preincubation protocol). Poly(*N*-[2-(α-D-mannopyranosyl-oxy)ethyl] methacrylamide) (PEMM, M_n = 53600 kg mol^{-1} and $Đ$ = 1.17), a mannosylated glycopolymer with a short ethyl linker, was also tested to evaluate the influence of the alkyl spacer on bacterial adhesion inhibition (structure given in Scheme 2). T84 cells were selected due to their high level of expression of CEACAM6 glycoprotein, an established receptor for AIEC bacteria adhesion on intestinal host cells in Crohn's disease patients.[36] Preincubation assays were primarily performed at 0.1 μM (on mannose unit basis) of FimH antagonists (Figure 3A). Levels of AIEC LF82 bacteria adhering to the cells in the presence of antagonists were expressed in percentages of residual bacteria, 100% corresponding to adhesion in absence of any compound. At such concentrations, no monovalent reference efficiently impedes the binding of AIEC LF82 to T84 cells (residual adhesion over 80% for α-D-mannose and HM) even though noticeable decrease of adhesion level is observed with HMM (59%). In the presence of the multivalent PHMM chains, the residual percentage of AIEC LF82 bound to T84 cells considerably drops (levels of adhesion typically ranging from 17 to 43%). Inhibitory activities tend to increase with chain length for linear glycopolymers (39, 23, and 17% for L31, L106, and L188, respectively) and to slightly decrease with the number of arms for the star-shaped glycopolymers (20 and 26% for T200 and O269). More generally, consistent with previous work of Stenzel and co-workers on concanavaline A and glucosylated polymers, no enhancement of activity is observed for star-shaped glycopolymers.[37] In contrast to PHMM, PEMM shows no inhibitory activity at 0.1 μM (Figure S4). This result confirms that the presentation of multiple binding sites on a polymer scaffold is not sufficient for designing effective antiadhesive polymers and that optimization of the interactions between the ligand and the binding pocket within the FimH adhesin domain is of crucial importance.[20] Dose-dependent effects were further explored for several compounds of each polymer group (L31, L188, T51, T200, O98, and monovalent ligands as references, see Figure 3C). No significant antiadhesive properties were observed below a concentration of 1 μM for monovalent mannosides (HMM, HM). Polymer ligands, especially linear and 3-arm stars PHMM, display greater inhibitory activity than monovalent ligands, whereas 1 μM of HMM, the most effective monovalent ligand, is required to inhibit significantly the attachment of AIEC LF82 to T84 cells (residual adhesion 45%), the presence of 10 nM of PHMM with the highest valency (L188 or T200) results in similar levels of adhesion (45 and 50%). This 100× increase in inhibitory potency (valency-corrected) clearly highlights the benefits of multivalent polymeric inhibitors over monovalent ligands.

Postincubation experiments were subsequently performed to evaluate the aptitude of HM-based compounds to disrupt pre-established interactions between T84 intestinal epithelial cells and AIEC LF82 bacteria (Figure 3B,D). Thus, T84 cells were first infected by bacteria, extensively washed to eliminate nonadhering bacteria and subsequently incubated with monovalent or macromolecular FimH antagonists for 3 h. No efficient detachment of bacteria was observed upon addition of molecular inhibitors with less than 10 μM (55 and 67% of residual adhesion for HM and HMM). In contrast, the majority of AIEC bacteria are washed out when a concentration of 0.1 μM (on mannose basis) of the most potent glycopolymers is added (36, 47, and 43% of residual adhesion for L31, L188, and T200). These results demonstrate that PHMM chains are not only capable to efficiently inhibit recognition events in a prophylactic approach but also to disrupt established

DOI: 10.1021/acs.biomac.5b00413
Biomacromolecules 2015, 16, 1827−1836

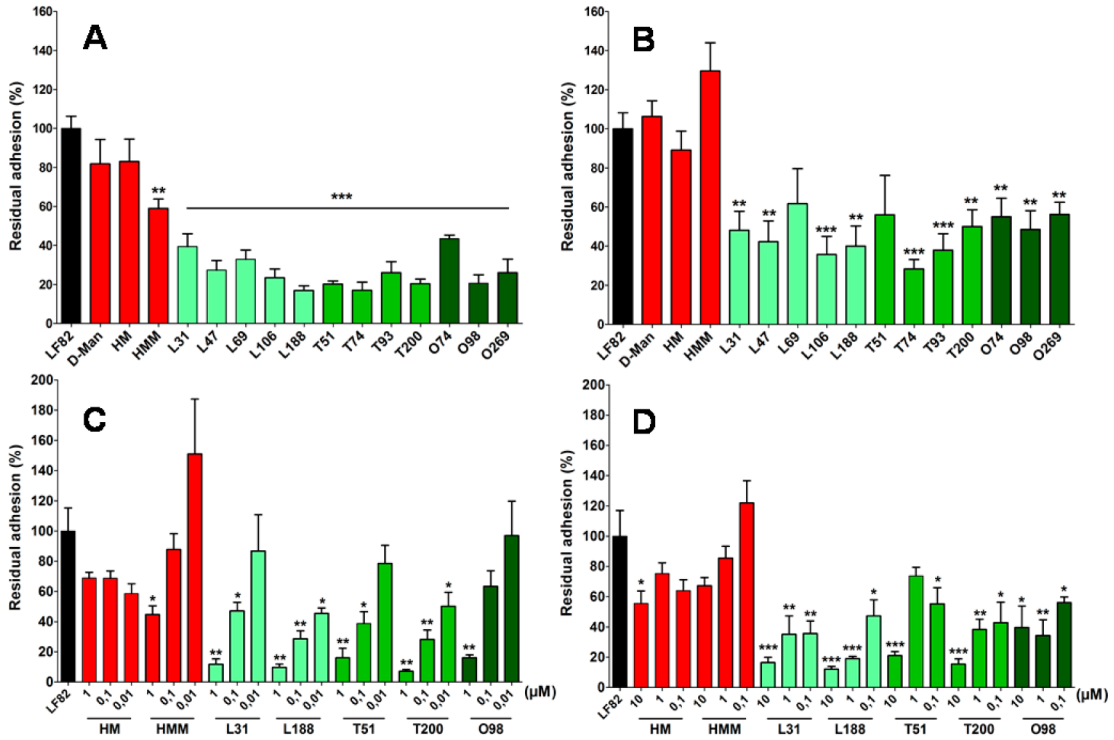

Figure 3. (A) Residual adhesion of the bacterial strain AIEC LF82 to T84 cells at a concentration of 0.1 μM of inhibitors (on mannose unit basis) in preincubation experiments. (B) Residual adhesion of the bacterial strain AIEC LF82 to T84 cells at a concentration of 1 μM of inhibitors (on mannose unit basis) in postincubation experiments. (C) Inhibitory effects of mannosides or glycopolymers (at 0.01, 0.1, and 1 μM) on AIEC LF82 adhesion levels to T84 cells in preincubation experiments. (D) Inhibitory effects of mannosides or glycopolymers (at 0.1, 1, and 10 μM) on AIEC LF82 adhesion levels to T84 cells in postincubation experiments. Results are expressed as percentages of adherent bacteria, AIEC LF82 adhesion in the absence of inhibitors, was considered as 100% (mean ± SEM). *P < 0.05, **P < 0.01, ***P < 0.001.

interactions between epithelial cell receptors and FimH adhesion domains.

Based on the pre- and postincubation assays data, L188 was finally selected for testing PHMM antiadhesive properties in ex vivo conditions. More specifically, the ability of this macromolecular antagonist to prevent AIEC LF82 adhesion was tested on a model of colonic loops of transgenic CEABAC10 mice expressing CEACAM6. With that aim, LF82 bacteria (6×10^5 CFU) or a mix of LF82 bacteria (6×10^5 CFU) and L188 (3.4 μmol of mannose units) were injected into the loops and incubated for 1 h. After washing steps, LF82 adhesion levels to the intestinal tissue in the presence or absence of inhibitor were estimated (see Figure 4). As observed in vitro on T84 cells, L188 actively prevents AIEC attachment to the colonic tissues (6.4×10^6 CFU/g of tissue for PHMM-free experiment vs 2.5×10^6 CFU/g of tissue in the presence of PHMM, 61% decrease of bacteria adhering to colonic mucosa).

Competitive enzyme-linked lectinosorbent assays (ELLSA) were finally carried out to gain further knowledge on the association of the glycopolymers to FimH (as a function of the HM valency and topology). Briefly, the principle of this assay lies in the competition between FimH/glycopolymers and FimH/RNaseB interactions, RNaseB being a protein (coated on the immunosorbent plates) that displays a mixture of oligomannose glycans ($Man_5GlcNAc_2$, $Man_7GlcNAc_2$, and $Man_8GlcNAc_2$) capable of strongly binding to FimH (see technical details in the Supporting Information). The intensity of FimH binding to the substrate represented by the optical density of chromophore absorbance at 450 nm was measured for a dilution series of glycopolymers as well as for α-D-mannose,

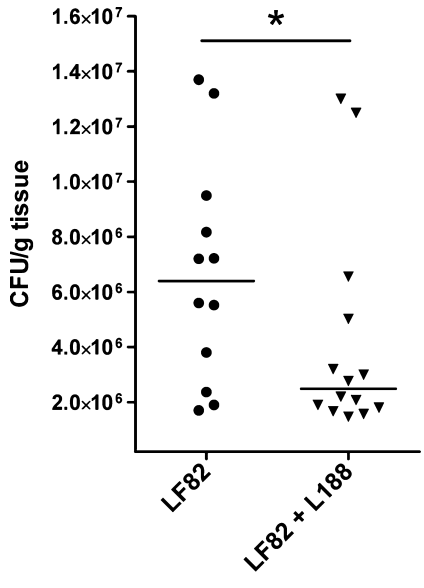

Figure 4. Inhibitory effect of glycopolymer L188 on the adhesion level of the AIEC LF82 strain to intestinal tissue from transgenic CEABAC10 mice expressing human CEACAM6. Bacteria were preincubated 15 min with the inhibitor at a dose of 3.4 μmol of mannose units, then a volume of 100 μL of bacteria/inhibitor mixture was injected into colonic loops (~0.6 cm for 1 h). Results are expressed as percentages of bacteria adherent to the colonic mucosa (mean ± SEM, n = 5−8 mice). A total of 100% corresponds to the bacterial adhesion in the absence of any treatment (NT for nontreated); *P < 0.05.

DOI: 10.1021/acs.biomac.5b00413
Biomacromolecules 2015, 16, 1827−1836

methyl α-D-mannoside, and HM as molecular references to build dose−response inhibition profiles (see Figure S5). In contrast to the conclusions drawn from the adhesion tests, the highest level of inhibition (IC_{50} = 0.11 μM) was obtained for HM. Thanks to the favored binding of FimH to pendent HM ligands, the glycopolymers also efficiently disrupt FimH/RNaseB association but no gain of affinity is observed with macromolecular inhibitors (IC_{50} = 0.40−1.5 μM Man) owing to the monovalent nature of the FimH binding site. The apparent affinity of the pendent HM bound to the polymeric structure is indeed lower than the one observed for the free HM reference probably due steric hindrance. As a general trend, the activity of the glycopolymers (on a mannose unit basis) slightly decreases with DP_n, whereas topology has barely any influence. Importantly, the glycopolymer chains still display considerably higher affinity for FimH than α-D-mannose or methyl α-D-mannoside (IC_{50} = 38.4 and 12 μM, respectively), confirming the importance of the heptyl group between the mannosides and the polymer backbone. Taken together, these results suggest that the significant enhancement in activity over monovalent ligands (highlighted by the antiadhesive tests) is not related to a higher intrinsic affinity of the polymer bound ligands for FimH, but to the capability of the glycopolymers to undergo multiple cross-linking interactions with living bacteria and to generate large aggregates in which only peripheral bacteria can adhere to the cells.

CONCLUSIONS

We have evaluated the potential interest of the multivalent approach in preventing/disrupting Adherent Invasive *E. coli* adhesion implied in Crohn's disease inflammation. A series of precisely defined linear and star-shaped glycopolymers bearing multiple pendent copies of HM and having different chain length has first been designed. Investigation of AIEC strain LF82 adhesion to T84 cells in the presence of molecular and macromolecular antagonists highlighted the remarkable anti-adhesive capacities of HM-based glycopolymers in vitro. Compared to the monovalent HM reference, HM-based glycopolymers were more than 100-fold more potent (valency corrected basis) in preventing/disrupting AIEC attachment to intestinal epithelial cells. The antiadhesive effect was further evidenced ex vivo, in the colon of a transgenic mouse model of CD. As evidenced by the lower IC_{50}s observed for macromolecular inhibitors in ELLSA assays performed with recombinant FimH, the enhancement in activity is not due to a greater intrinsic affinity for FimH targets but rather to cross-linking interactions and aggregation of the bacteria as suggested by DLS and fluorescence microscopy analyses on HM-based glycopolymers and FimH and bacteria/glycopolymer mixtures. These disparities between ELLSA and adhesion assays also indicate that, in the quest for highly efficient pathogen anti-adhesives, classically performed carbohydrate−lectin interaction studies, such as ELLSA, ITC, or SPR, should be interpreted with caution when they do not account for pathogen aggregation that significantly impact the cell-adhesive properties. Importantly, the in vitro and ex vivo results reported here illustrate the strong potential of the multivalent concept to prevent/disrupt AIEC attachment to the gut and constitute a step further toward an antiadhesive treatment of *E. coli*-induced inflammatory diseases.

ASSOCIATED CONTENT

Supporting Information

Kinetics of polymerization, glycopolymer characterizations, NMR spectra of CTAs and glycopolymers, cytotoxicity tests, adhesion tests for PEMM, principle and results of the ELLSA tests and DLS of FimH/glycopolymers mixtures. The Supporting Information is available free of charge on the ACS Publications website at DOI: 10.1021/acs.biomac.5b00413.

AUTHOR INFORMATION

Corresponding Authors

*E-mail: julien.bernard@insa-lyon.fr. Fax: 0033472438527.
*E-mail: julie.bouckaert@univ-lille1.fr.
*E-mail: sebastien.gouin@univ-nantes.fr.

Author Contributions

‡These authors equally contributed to this work (X.Y. and A.S.).

Notes

The authors declare no competing financial interest.

ACKNOWLEDGMENTS

X.Y. acknowledges the Chinese Scholarship Council for a Ph.D. grant. T.D. and R.B. acknowledge for the West Ukrainian BioMedical Center grants and the grant of the President of Ukraine. This work was carried out with financial support from the French Agence Nationale de la Recherche (ANR Programme Blanc STARLET, ANR-12-BSV5-0016-01), the Ministère de la Recherche et de la Technologie, Inserm (UMR 1071) and INRA (USC-2018).

DEDICATION

†This paper is dedicated to the memory of our dear colleague Arlette Darfeuille-Michaud who recently passed away.

REFERENCES

(1) Choudhury, D.; Thompson, A.; Stojanoff, V.; Langermann, S.; Pinkner, J.; Hultgren, S. J.; Knight, S. D. *Science* **1999**, *285*, 1061−1066.
(2) Sharon, N. *Biochim. Biophys. Acta* **2006**, *1760*, 527−537.
(3) Firon, N.; Ashkenazi, S.; Mirelman, D.; Ofek, I.; Sharon, N. *Infect. Immun.* **1987**, *55*, 472−476.
(4) Bouckaert, J.; Berglund, J.; Schembri, M.; De Genst, E.; Cools, L.; Wuhrer, M.; Hung, C. S.; Pinkner, J.; Slattegard, R.; Zavialov, A.; Choudhury, D.; Langermann, S.; Hultgren, S. J.; Wyns, L.; Klemm, P.; Oscarson, S.; Knight, S. D.; De Greve, H. *Mol. Microbiol.* **2005**, *55*, 441−455.
(5) Han, Z. F.; Pinkner, J. S.; Ford, B.; Obermann, R.; Nolan, W.; Wildman, S. A.; Hobbs, D.; Ellenberger, T.; Cusumano, C. K.; Hultgren, S. J.; Janetka, J. W. *J. Med. Chem.* **2010**, *53*, 4779−4792.
(6) Han, Z. F.; Pinkner, J. S.; Ford, B.; Chorell, E.; Crowley, J. M.; Cusumano, C. K.; Campbell, S.; Henderson, J. P.; Hultgren, S. J.; Janetka, J. W. *J. Med. Chem.* **2012**, *55*, 3945−3959.
(7) Klein, T.; Abgottspon, D.; Wittwer, M.; Rabbani, S.; Herold, J.; Jiang, X. H.; Kleeb, S.; Luthi, C.; Scharenberg, M.; Bezencon, J.; Gubler, E.; Pang, L. J.; Smiesko, M.; Cutting, B.; Schwardt, O.; Ernst, B. *J. Med. Chem.* **2010**, *53*, 8627−8641.
(8) Jiang, X. H.; Abgottspon, D.; Kleeb, S.; Rabbani, S.; Scharenberg, M.; Wittwer, M.; Haug, M.; Schwardt, O.; Ernst, B. *J. Med. Chem.* **2012**, *55*, 4700−4713.
(9) Sperling, O.; Fuchs, A.; Lindhorst, T. K. *Org. Biomol. Chem.* **2006**, *4*, 3913−3922.
(10) Brument, S.; Sivignon, A.; Dumych, T. I.; Moreau, N.; Roos, G.; Guerardel, Y.; Chalopin, T.; Deniaud, D.; Bilyy, R. O.; Darfeuille-Michaud, A.; Bouckaert, J.; Gouin, S. G. *J. Med. Chem.* **2013**, *56*, 5395−5406.

DOI: 10.1021/acs.biomac.5b00413
Biomacromolecules 2015, 16, 1827−1836

(11) Darfeuille-Michaud, A.; Neut, C.; Barnich, N.; Lederman, E.; Di Martino, P.; Desreumaux, P.; Gambiez, L.; Joly, B.; Cortot, A.; Colombel, J. F. *Gastroenterology* **1998**, *115*, 1405−1413.
(12) Darfeuille-Michaud, A.; Boudeau, J.; Bulois, P.; Neut, C.; Glasser, A. L.; Barnich, N.; Bringer, M. A.; Swidsinski, A.; Beaugerie, L.; Colombel, J. F. *Gastroenterology* **2004**, *127*, 412−421.
(13) Boettner, B. *SciBX* **2013**, *6*, 1−2.
(14) Bernardi, A.; Jimenez-Barbero, J.; Casnati, A.; De Castro, C.; Darbre, T.; Fieschi, F.; Finne, J.; Funken, H.; Jaeger, K. E.; Lahmann, M.; Lindhorst, T. K.; Marradi, M.; Messner, P.; Molinaro, A.; Murphy, P. V.; Nativi, C.; Oscarson, S.; Penades, S.; Peri, F.; Pieters, R. J.; Renaudet, O.; Reymond, J. L.; Richichi, B.; Rojo, J.; Sansone, F.; Schaffer, C.; Turnbull, W. B.; Velasco-Torrijos, T.; Vidal, S.; Vincent, S.; Wennekes, T.; Zuilhof, H.; Imberty, A. *Chem. Soc. Rev.* **2013**, *42*, 4709−4727.
(15) Becer, C. R. *Macromol. Rapid Commun.* **2012**, *33*, 742−752.
(16) Kanain, M.; Mortell, K. H.; Kiessling, L. L. *J. Am. Chem. Soc.* **1997**, *119*, 9931−9932.
(17) Kitov, P. I.; Sadowska, J. M.; Mulvey, G.; Armstrong, G. D.; Ling, H.; Pannu, N. S.; Read, R. J.; Bundle, D. R. *Nature* **2000**, *403*, 669−672.
(18) Kitov, P. I.; Mulvey, G. L.; Griener, T. P.; Lipinski, T.; Solomon, D.; Paszkiewicz, E.; Jacobson, J. M.; Sadowska, J. M.; Suzuki, M.; Yamamura, K. I.; Armstrong, G. D.; Bundle, D. R. *Proc. Natl. Acad. Sci. U.S.A.* **2008**, *105*, 16837−16842.
(19) Kumar, J.; McDowall, L.; Chen, G.; Stenzel, M. H. *Polym. Chem.* **2011**, *2*, 1879−1886.
(20) Richards, S.-J.; Jones, M. W.; Hunaban, M.; Haddleton, D. M.; Gibson, M. I. *Angew. Chem., Int. Ed.* **2012**, *51*, 7812−7816.
(21) Polizzotti, B. D.; Kiick, K. L. *Biomacromolecules* **2006**, *7*, 483−490.
(22) Grunstein, D.; Maglinao, M.; Kikkeri, R.; Collot, M.; Barylyuk, K.; Lepenies, B.; Kamena, F.; Zenobi, R.; Seeberger, P. H. *J. Am. Chem. Soc.* **2011**, *133*, 13957−13966.
(23) Pasparakis, G.; Cockayne, A.; Alexander, C. *J. Am. Chem. Soc.* **2007**, *129*, 11014−11015.
(24) Lundquist, J. J.; Toone, E. *Chem. Rev.* **2002**, *102*, 555−578.
(25) Lindhorst, T. K.; Kieburg, C.; Krallmann-Wenzel, U. *Glycoconjugate J.* **1998**, *15*, 605−613.
(26) Nagahori, N.; Lee, R. T.; Nishimura, S.-I.; Pagé, D.; Roy, R.; Lee, Y. C. *ChemBioChem* **2002**, *3*, 836−844.
(27) Touaibia, M.; Wellens, A.; Shiao, T. C.; Wang, Q.; Sirois, S.; Bouckaert, J.; Roy, R. *ChemMedChem* **2007**, *2*, 1190−1201.
(28) Gouin, S. G.; Wellens, A.; Bouckaert, J.; Kovensky, J. *ChemMedChem* **2009**, *4*, 749−755.
(29) Almant, M.; Moreau, V.; Kovensky, J.; Bouckaert, J.; Gouin, S. G. *Chem.—Eur. J.* **2011**, *17*, 10029−10038.
(30) Bouckaert, J.; Li, Z. L.; Xavier, C.; Almant, M.; Caveliers, V.; Lahoutte, T.; Weeks, S. D.; Kovensky, J.; Gouin, S. G. *Chem.—Eur. J.* **2013**, *19*, 7847−7855.
(31) Yan, X.; Delgado, M.; Fu, A.; Alcouffe, P.; Gouin, S. G.; Fleury, E.; Katz, J. L.; Ganachaud, F.; Bernard, J. *Angew. Chem., Int. Ed.* **2014**, *53*, 6910−6913.
(32) Datsenko, K. A.; Wanner, B. L. *Proc. Natl. Acad. Sci. U.S.A.* **2000**, *97*, 6640−6645.
(33) Li, Z.; Bouckaert, J.; Deboeck, F.; De Greve, H.; Hernalsteens, J. P. *Microbiology* **2012**, *158*, 736−745.
(34) Bathfield, M.; D'Agosto, F.; Spitz, R.; Charreyre, M.-T.; Delair, T. *J. Am. Chem. Soc.* **2006**, *128*, 2546−2547.
(35) Chan, C. H.; Stanners, C. P. *Mol. Ther.* **2004**, *9*, 775−785.
(36) Barnich, N.; Carvalho, F. A.; Glasser, A.-L.; Darcha, C.; Jantscheff, P.; Allez, M.; Peeters, H.; Bommelaer, G.; Desreumaux, P.; Darfeuille-Michaud, A. *J. Clin. Invest.* **2007**, *117*, 1566−1574.
(37) Chen, Y.; Chen, G.; Stenzel, M. H. *Macromolecules* **2010**, *43*, 8109−8114.

DOI: 10.1021/acs.biomac.5b00413
Biomacromolecules 2015, 16, 1827−1836